Int J Adv Manuf Technol (2017) 92:247–258
DOI 10.1007/s00170-017-0120-9

ORIGINAL ARTICLE

Using Barkhausen noise to measure coating depth of coated high-speed steel

N. Seemuang[1] · **T. Slatter**[1]

Received: 31 August 2016 / Accepted: 1 February 2017 / Published online: 22 February 2017

Abstract Coated high-speed steel tools are widely used in machining processes as they offer an excellent tool life to cost ratio, but they quickly need replacing once the coated layer is worn away. It would be therefore useful to be able to measure the tool life remaining non-destructively and cheaply. To achieve this, the work presented here aims to measure the thickness of the coated layer of high-speed cutting tools by using Barkhausen noise (BHN) techniques. Coated high-speed steel specimens coated with two different materials (chromium nitride (CrN), titanium nitride (TiN)) were tested using a cost-effective measuring system developed for this study. Sensory features were extracted from the signal received from a pick-up coil and the signal features, Root mean square, peak count, and signal energy, were successfully correlated with the thickness of the coating layer on high-speed steel (HSS) specimens. The results suggest that the Barkhausen noise measuring system developed in this study can successfully indicate the different thickness of the coating layer on CrN/TiN coated HSS specimens.

Keywords Barkhausen noise · Coating · High-speed steel

✉ T. Slatter
tom.slatter@sheffield.ac.uk

N. Seemuang
nseemuang1@sheffield.ac.uk

[1] Department of Mechanical Engineering, University of Sheffield, Mappin St., Sheffield S1 3JD, UK

1 Introduction

Coated tools are commonly used in machining processes (e.g. titanium nitride (TiN) coated high-speed steel (HSS) for gear hob cutters) as they offer longer tool life and promote good machinability of the workpiece when compared with uncoated tools [1]. During production operations assessment of the remaining coating depth of coated tools could be helpful information for the machine operator to avoid using an excessively worn tool.

Tool wear measurements are also routinely taken when conducting research in this area, for example in tool geometry [2, 3] or microstructural design [4, 5], or considering the role of different cutting conditions [6, 7]. A number of different techniques are often used to evaluate tool wear, irrespective of the surface treatment or coating used, for example optical methods [8, 9], acoustic emission detection [10–12], ultrasonic testing [13, 14], and thermal/infrared measurements [15, 16]. The cost and characteristics of each technique should be considered in order to ensure the best fit for a given monitoring purpose and application.

Techniques reliant on the evaluation of the magnetic/electromagnetic properties of the tools are less widely used. One such technique, known as Barkhausen noise (BHN), has been variously investigated with a view to using it to assess material deformation, fatigue, grinding burn evaluation, and interestingly for this work, the measurement of case-depth. It has been found that BHN activity (peak amplitude and signal energy) increases significantly with tensile stress, and decrease under compressive stress [17]. As also found in Moorthy et al., Vincent et al. and Lindgren and Lepistö [17–19], BHN can be used to classify the different stages of fatigue because BHN activity appears to increase in the first stage

of fatigue, decreases in second stage, and increases again in final stage. As BHN can also be applied in grinding burn detection as found in the study of Moorthy et al., Wilson et al. and Sorsa et al. [20–22]. They used low and high frequency measuring systems to detect grinding burn. A single-peaked BHN profile obtained by high frequency measurements can be well correlated with the residual stress change due to grinding burn.

Heat treatments such as carburising and induction hardening are normally used to create a hard and a wear resistant layer on top of the softer substrate. These processes can change the metallurgical properties of the workpiece at a certain depth below the surface. In the case of a tool, the presence of this layer is crucial to its performance, and therefore assessment of the layer depth can be used to evaluate the remaining life. Metallographic analysis, subsurface micro-hardness measurement after cross-sectioning, and direct carbon content evaluation by chemical or spectrographic methods, are normally used to evaluate the case-depth [23]. These methods are destructive, are time-consuming to perform, and clearly cannot be used to evaluate any progressive reduction in the case depth 87 of a tool during its use [24]. This demonstrates the need of a reliable and non-destructive method for the case-depth measurement either online or offline between instances of the tool being used.

Generally, the evaluation of case depth can be performed by BHN measurement and based on the hardness difference of the hardened case and the soft core of the material [25]. Several studies concluded that two-peaked BHN profiles are obtained when the hardening depth is measured by BHN technique [26–28]. It is found that the first peak at a lower applied field strength corresponds to the soft core and the second peak corresponding to the hardened case. The ratio of these two peaks can be used to represent the case-depth but the two peak profiles are not always found, as reported by Moorthy et al. and Dubois and Fiset [27, 29]. Moorthy et al. also observed that the second peak cannot be found if the case depth is too deep, and they suggested that the two peak profiles can be found when the case depths up to 1 mm, and then case depth can be determine by the ratio of two peak heights [27]. To increase sensitivity of BHN profile, Blaow and Shaw suggested that an increase of the excitation field strength can increase the height of both peaks. The peak at a higher field increases significantly compared to one at lower field [30].

It is possible that the hardened surface undergoes a decarburising process where the surface layer softens. Conversely, a single-peaked profile transforms into a two-peaked one where decarburisation occurs as reported in Blaow and Shaw [31]. In addition, the height of the second peak at higher applied field strengths increased with increasing depths and the peak position shifted to lower field strengths. According to Stapakov et al. [32], the root mean square (RMS) value first increases, then followed by a decrease with an increasing depth of the decarburised layer.

The case-depth of many steel types treated by carburising and nitriding was studied by Dubois et al. [29]. The BHN technique was used to evaluate case-depth of carburised steels (AISI 8620 and 9310) and nitride tool steels (AISI P20, D2, and H13). They used the frequency spectrum to find the correlation between the frequency content and case depth. The results showed good correlation between BHN and hardening depth values of the order of 100 and 1000 μm for carburised steels, and 25 and 200 μm for nitride steels.

Wilson et al. applied magneto-acoustic emission (MAE) and magnetic Barkhausen emission (MBE) to measure case depth in EN36 gear steels [21]. This study showed that the overall amplitudes of both MBE and MAE have a good relation with the case depth. They concluded that the peak amplitude decreases with an increase of case depth. Santa-aho et al. [33] observed the same relationship between the RMS value and the case depth. They also proposed a new approach to detect the case depth by using voltage and frequency sweeps to evaluate the thickness of the surface layer. The BHN magnetising sweeps technique was used to measure the case-depth in hardened steel. The results from magnetising voltage sweeps (MVS) were analysed and compared to the case-depths from conventional method. It is observed that the ratio of two voltage sweeps with different frequencies produces a good estimation of the case depth. Drehmer et al. [34] applied BHN measurement for estimating the case depth of SAE 1020 steel. They used RMS Barkhausen pulse envelope and fast Fourier transforms (FFT) to estimate case depths. Successfully, the normalised power index (NPI) was proposed to estimate case depths if the properties of the surface layer and core are considerably different.

It appears that work investigating applications of BHN is sporadic but there is enough to hypothesise that the technique may be able to measure the presence of coatings if the characteristic difference between the coating and the substrate can be considered analogous to the difference between a case hardened layer and soft core. Success may, however, be limited by the target material system being non-ferromagnetic (the coating) paired with ferromagnetic (the substrate), rather than a single ferromagnetic material with microstructural variants (nominally the case hardened layer and the soft core). That said, it is still a worthwhile endeavour to evaluate the use of this non-destructive technique to monitor coated layer in coated high-speed cutting tool as in a similar fashion to the use of magnetic methods to measure case hardening.

This study aims to propose a suitable methodology for measuring the coated layer depth of coated cutting tools using BHN measurements. The relationship between BHN features and the coating layer depth in the HSS specimens was studied, as this is an important issue for future research on tool condition monitoring.

2 Experimental setup and procedure

2.1 Specimen preparation

The specimens used in this study were manufactured from M2 grade high-speed steel with the composition shown in Table 1. The specimens had dimensions of 25 × 50 × 5 mm and were coated with three different thicknesses (nominally 5, 10 and 15 μm) of either chromium nitride (CrN, silver colour) or titanium nitride (TiN, gold colour), or left uncoated (Fig. 1). The coated specimens were prepared by electron beam plasma assisted physical vapour deposition (EBPA-PVD) and the process temperature was 450 °C with 10×10^{-3} mbar of process pressure. The thickness of coated layers were measured by X-ray fluorescence (Fischerscope XRF) and were as listed in Table 2.

2.2 Equipment

The experimental setup of the BHN measuring system developed for this work is shown in Fig. 2. A National Instruments USB-6212 *(a)* was used for generating the exciting current signal to a magnetic yoke *(c)* at specific exciting frequency (fe) controlled by LabVIEW. This exciting signal was then magnified by bipolar power amplifier *(b)* to gain current signal up to 1 A for the exciting coil *(c)* made from copper wire wound around the Fe-Si lamination core. A current probe *(d)* was used to monitor the exciting current, the actual current in the exciting coil to determine the magnetic field strength (*H*) to the workpiece, and also for damage prevention due to over current.

The magnetic flux from the excited coil flows through the specimen via the yoke's poles. A search coil or pick-up coil *(e)*, picks up the BHN signal from the specimen. The relatively low level of BHN signal was gained by custom design signal amplifier *(f)* to a suitable level for subsequent signal processing. All signals were gained and filtered *(g)* before processing the signals via a personal computer interfaced by a National Instruments NI-9223 *(h)*. Post signal processing and feature extraction was performed by Matlab.

2.3 Experimental methodology/signal processing and feature extraction

The applied current to magnetic yoke was varied from 0.1 to 1 A to induce different magnetic field strengths (H) to pass through the specimens being examined. Then, the pick-up coil detects the BHN signal. The BHN signal was sampled at 200 kS/s with 70 dB of amplification gain. The raw signal was first filtered by high-pass filter at 1 kHz of the cut-off frequency to remove unwanted frequencies. The signal of each measurement was collected for 5 s. For the sensory feature extraction process, the signals generated within two complete magnetising cycles were used in the calculation; however, to eliminate a contamination of other unexpected noises at the beginning of a measurement, only signals collected after 1 s were selected.

Table 1 Composition (% by weight), HSS (M2)

Fe	C	Si	Mn	P	S
Balance	0.78/1.05	0.20/0.45	0.15/0.40	0.03	0.03
Cr	Mo	Ni	W	V	Cu
0.20/0.45	4.50/5.50	0.3	5.50/6.75	1.75/2.20	0.25

The typical BHN signal (in the time domain) received from the pickup coil is shown in Fig. 3a, and the frequency bandwidth of the BHN signal is in the range of 0.5–6 kHz as shown in Fig. 3b where the exciting frequency was set at 5 Hz.

In this study, only time-domain features were extracted from the selected signal, such as RMS, peak amplitude. In addition, peak count and signal energy (area under peaks) were also used as they could be used to indicate the intensity of a burst signal like that from BHN. The peak count and signal energy were calculated from the absolute signal amplitude as shown in Fig. 4a. The peak points of the BHN signal in Fig. 4b were counted if they are higher than the predefined threshold value and defined as 'peak count'. This feature was also used in the studies of Vashista and Moorthy [19] but they defined it as an 'event', and they used it to make an assessment of residual stress in the surface ground component.

Signal energy, defined as the area under the peaks of the absolute BHN signal amplitude over the fixed period, as shown in Fig. 4a, and it can be calculated by a graphical calculation method which also proposed by O'Sullivan et al. [137]. However, it can also be easily determined by trapezoidal numerical integration function in Matlab, and it was this numerical method used in this study.

Throughout this work, multiple measurements (at least three) were taken for each set of conditions (e.g. a particular applied current and frequency combination) used to measure each of the specimens listed in Table 2. These multiple measurements were very similar and repeatable to each other, and the data presented throughout "section 3" represents the signal(s) from one of these measurements and can be considered typical for the stated condition-specimen combination.

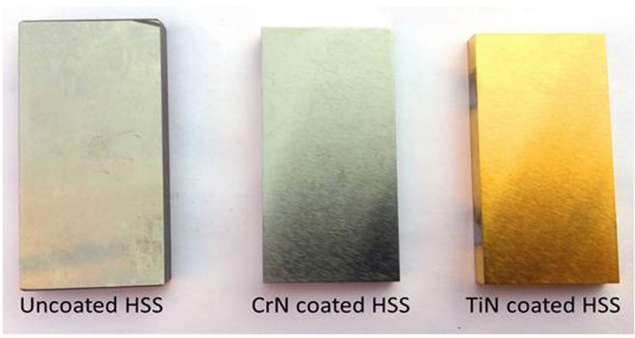

Fig. 1 CrN/TiN coated specimens with varying case-depth layer

Table 2 Coated HSS specimens used in this study

Coating materials	Thickness (μm)
CrN (5μm)	5.1
CrN (10μm)	10.9
CrN (15μm)	14.4
TiN (5μm)	5.0
TiN (10μm)	10.9
TiN (15μm)	14.4

3 Results and discussion

3.1 The influence of exciting frequency on uncoated high-speed steel specimen

To obtain the pick-up coil sensitivity and frequency response, a sinusoidal waveform was used to excite the magnetic flux in an uncoated HSS specimen, and the BHN signals acquired from the pick-up coils were then compared. These preliminary experiments were conducted in order to identify which excitation frequency and signal feature(s) would provide the highest likelihood of resolving any changes in the BHN signal when examining the differently prepared specimens.

The BHN signal received from the pick-up coil is shown in Fig. 5. The RMS value representing the signal amplitude of BHN signal continuously increases after 0.2 A of applied current and reaches the maximum values, and then decreases gradually. The RMS profiles of the lower exciting frequencies (Fig. 5a) are flatter than those of the higher exciting frequencies. This means that using a lower exciting frequency provides a wider measuring range of the BHN signal. The RMS values exhibit clearly-separated trends, while the peak amplitude has a fluctuating pattern (Fig. 5b). This oscillating trend of peak amplitude may be due to the interfering noises caused by unexpected events which contaminates to the main BHN signal such as an unexpected response of the electronics.

It is seen from Fig. 5 that the BHN signal induced by higher exciting frequency offers higher signal amplitude, which is represented by RMS and peak amplitude values (in the range of 0.2–0.4 A). This is due to higher rate of change in magnetisation and hence higher induced BHN voltage level. Conversely, a low exciting frequency produces a low rate of magnetisation and accordingly low induced voltage level received by the pick-up coil. These results are consistent with the finding of other studies [35], in which the high exciting frequency produces a higher BHN signal level than lower exciting frequency.

Comparing to different exciting frequencies in Fig. 5a, it can be observed the maximum of RMS values well correlates with the exciting frequency. Similar to the earlier studies that the positions of the peak RMS values are shifted from high values of applied current to low ones by an increasing of the exciting frequency [35, 36]. For example, the peak values of RMS profiles were found at applied currents of 0.7 A for 1 Hz, 0.5 A for 5 Hz, and 0.4 A for 10 Hz.

The completely-separated curve of BHN signal of each exciting frequency can be found by using the peak count and signal energy features (Fig. 6). The large number of peaks and signal energy can be found in 1 Hz excitation although the BHN voltage level is low.

It can therefore be concluded that the most useful features used for indicating the coating depth could be RMS, peak count and signal energy because they can well determine the differences in a BHN signal under different exciting frequencies in the range of 0.2–1 A, whereas peak amplitude can indicate only during 0.2–0.3 A of applied current.

The coated HSS specimens were then measured by the BHN system to investigate if the BHN measuring system was capable of measuring the coated HSS. In the first instance, the coated HSS specimens (both CrN and TiN) with the thickest depth (15 μm) were examined under different exciting frequencies.

The signal features shown in Fig. 7 confirm that the BHN signal in CrN/TiN-coated HSS can be detected by the BHN measuring system. Where compared with the results presented in Fig. 5, it appears that the BHN system can resolve the differences between the uncoated (Fig. 5a) and the coated HSS, through the value of features, the maximum value of

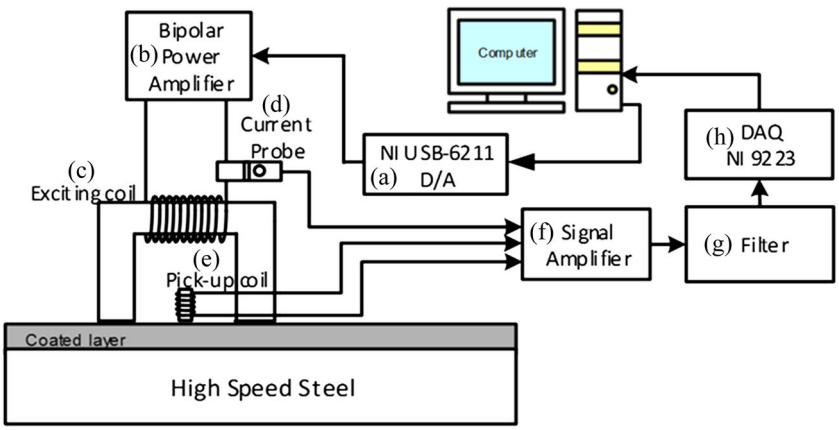

Fig. 2 Experimental setup

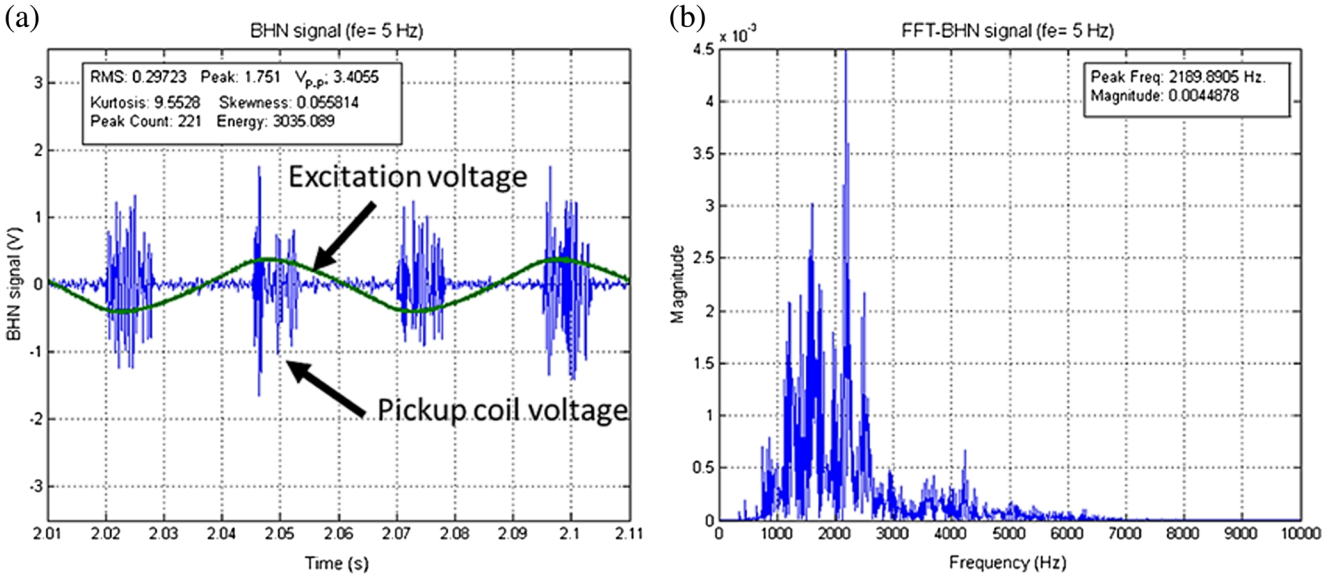

Fig. 3 **a** Typical excitation voltage and the BHN signals in time domain, and **b** typical frequency spectra of BHN signals acquired using pick-up coil in 1–6 kHz range

each feature in particular frequency, and the positions of those maximum values.

In summary, the RMS, peak count and signal energy can be used very well to indicate the differences between uncoated and coated HSS for each particular coating material under different exciting frequencies. The variations of those features can probably indicate the thickness of coating layer.

3.2 Comparison of coating depth on CrN-coated HSS

As the RMS value of the BHN signal appeared to be one of the most useful features to indicate the different thicknesses of the coating material on HSS, four coating thicknesses at different (increasing) exciting frequencies (Fig. 8a is 1 Hz, Fig. 8b is 5 Hz etc.) were first evaluated by the RMS values (Fig. 8).

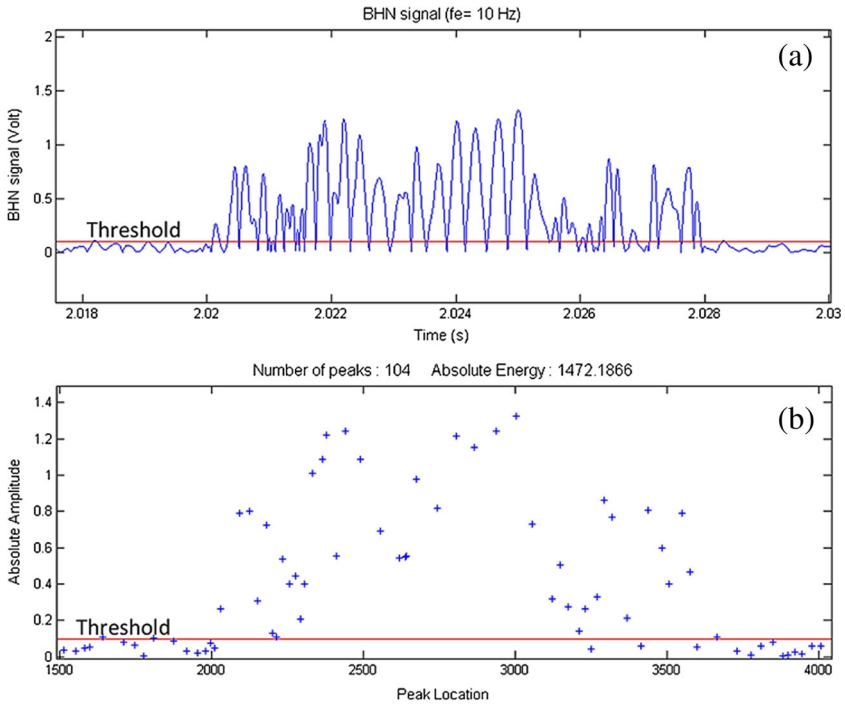

Fig. 4 Typical BHN signal of one burst **a** absolute amplitude and **b** the location of peaks over threshold value

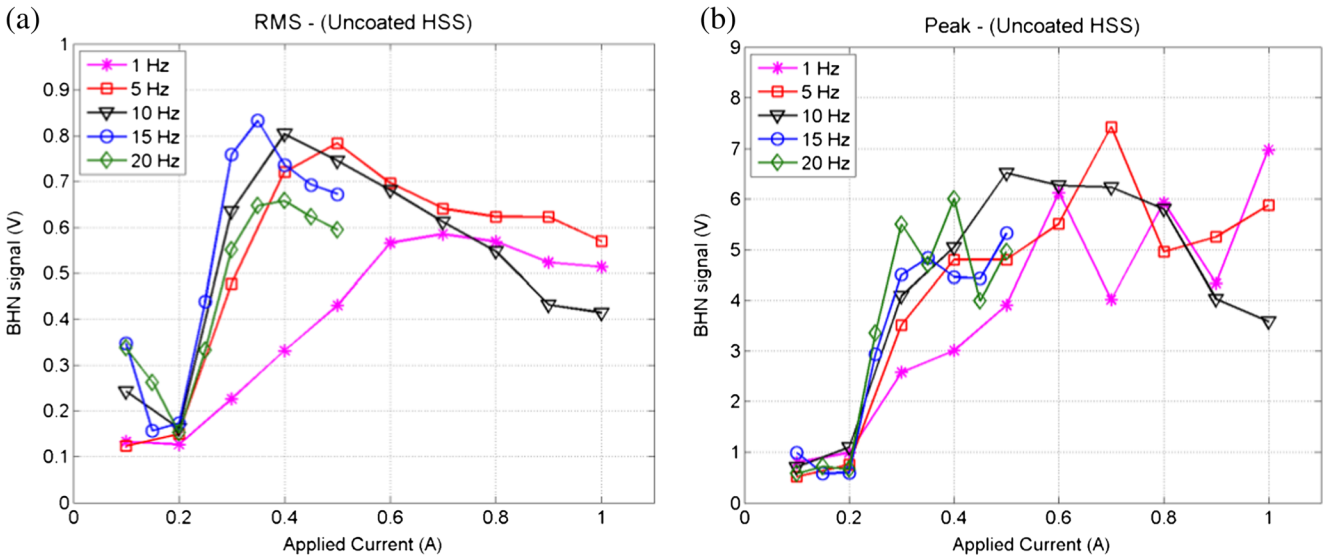

Fig. 5 BHN signal under different exciting frequency **a** RMS and **b** peak amplitude

The BHN signal of all exciting frequencies can be found after 0.2 A of applied current and the RMS values increase significantly until reach the maximum point (defined as BHN state I). The slope of the curve in this state correlates with the exciting frequency in which low exciting frequency in Fig. 8a provides low degree of slope (flatter), while high frequency (e.g. Fig. 8e) have a steeper slope. The RMS profiles in this state cannot be used to indicate the coating thickness because the RMS values for each coating thickness are difficult to distinguish. However, after reaching the maximum value (BHN state II), the RMS profiles are clearly separated and significantly oriented which could be used to indicate the thickness of coating layer for exciting frequency fe = 5, 10, 15, and 20 Hz. In case of fe = 1 Hz, the low frequency excitation induces deeper skin depth, therefore, a thin coating layer does not have a significant effect on the BHN signal levels (Fig. 8a). It can be clearly seen that the thicker coating layers have higher RMS values and thinner layers have lower RMS.

The exciting frequency has an influence on measurable range of the BHN signal. For example, the RMS feature can be used to indicate the coating thickness where the applied current varied between 0.6 and 1.0 A for the exciting frequency = 5 Hz, while it can be only used from 0.5 to 1.0 A in case of 10 Hz. In Fig. 8, the most useful exciting frequency appears to be 10 Hz because this frequency provides the largest measuring range (0.5–1.0 A) that can be used for coating depth measurement in CrN coated HHS, and the RMS profiles have more linearity than those in 5 Hz, which offers the same measuring range.

Similarly, the results presented in Fig. 9 confirm that peak count and signal energy features of 10 Hz can also be used to indicate the coating depth layer, while the peak amplitude

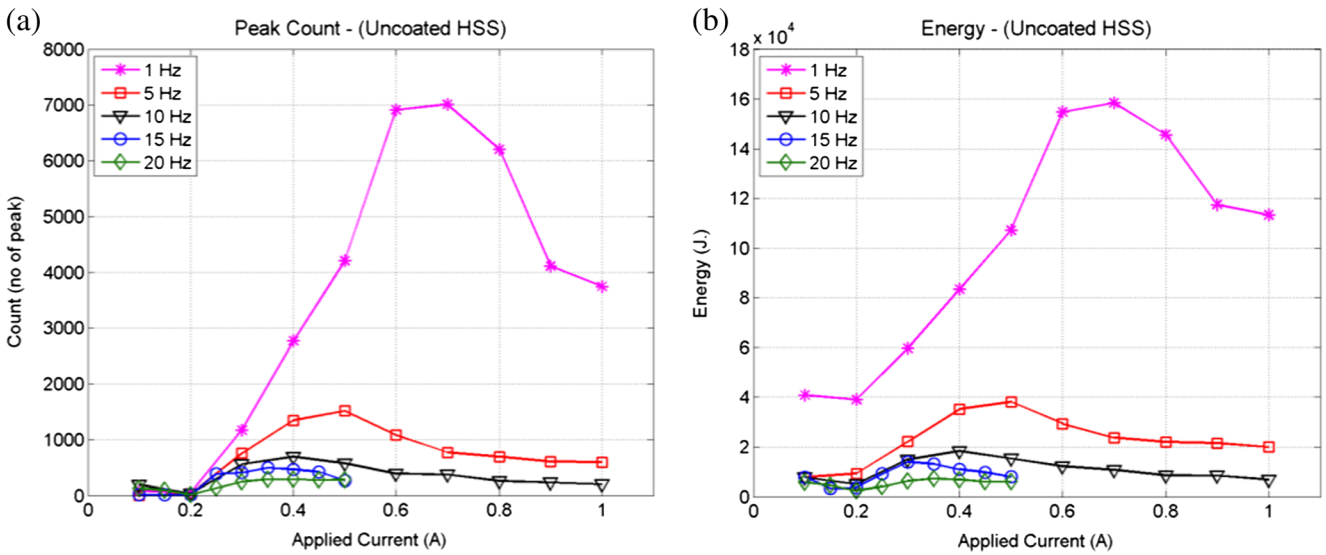

Fig. 6 BHN signal under different exciting frequency **a** peak count and **b** signal energy

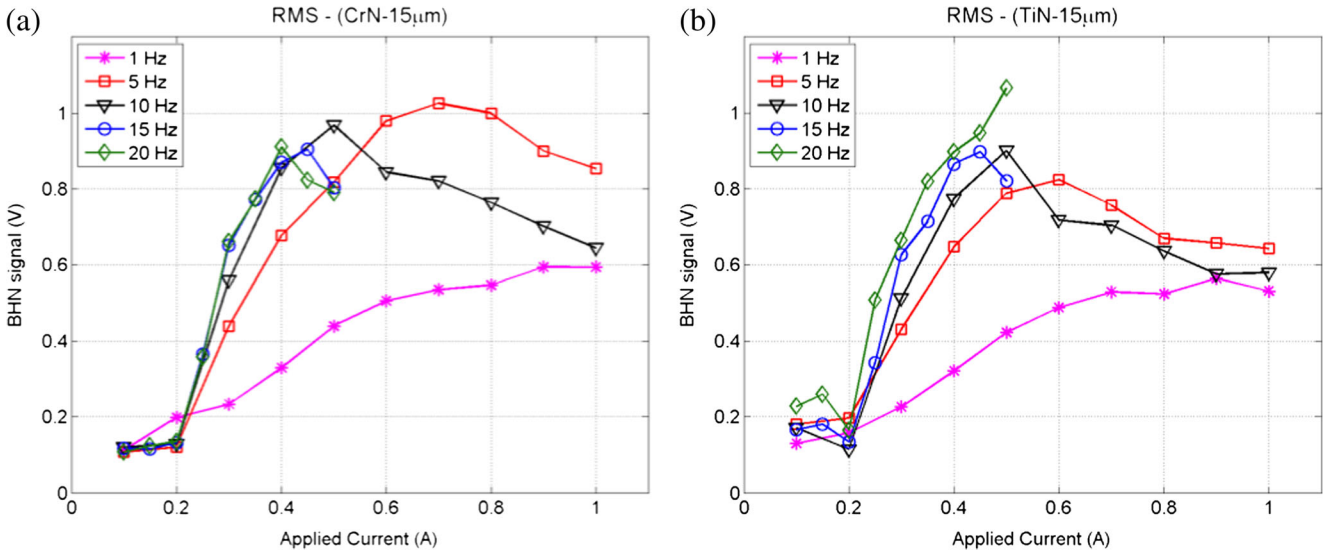

Fig. 7 RMS value measured from **a** CrN-coated HSS and **b** TiN-coated HSS

(Fig. 10) is unusable for indicating the difference of coating thickness due to unexpected noise. It is speculated that unexpected background noise or malfunctioning of the electronics in the measurement system would result in peak amplitude of BHN signal.

In conclusion, the effective magnetising conditions used for the propose BHN system in order to indicate the thickness of coating layer in CrN coated HSS are 10 Hz of exciting frequency and the applied current from 0.5 to 1 A. The effective features used to indicate the thickness of coating layer are RMS, peak count and signal energy.

3.3 Comparison of coating depth layer on TiN coated HSS

As in Fig. 8, Fig. 11 compares the RMS profiles of each exciting frequency for tests using TiN coated HSS. Similarly to the CrN coated specimens in Fig. 8, the RMS profiles are separated where the exciting frequency is greater than or equal to 5 Hz, but the separation is not in the expected order except for fe = 20 Hz.

The RMS profiles of each thickness in Fig. 11e have the correctly ordered separation from 0.2 A of applied current. It can also be confirmed by the peak count and signal energy features in Fig. 12 that this exciting frequency can be used to indicate the different thicknesses of TiN coated HSS. As before, it is important to note that the effective range of TiN coating depth measurement is quite specific and in the condition that applied current varies from 0.3 to 0.5 A, and the exciting frequency is equal to 20 Hz.

From the results, it can be concluded that the high exciting frequency offers very sensitive to near surface properties as offering a shallow skin depth due to the effect of lower magnetic field penetration and higher attenuation. Consequently, the coating layer will have a strong effect on the field penetration and the BHN signal, and accordingly the BHN signal, which has good correlation with the coating depth, can be detected in this case. In case of low frequency excitation, a thin coating layer would not significantly affect the BHN signal level since low frequency excitation induces deeper skin depth. Therefore, the variation in near surface properties does not have a significant effect on the BHN signal generation.

3.4 Evaluation of proposed methodology

From these results, it is shown that it is feasible to use the Barkhausen noise technique for measuring the coating depth layer on coated HSS cutting tools, especially the TiN coated HSS that is commonly used in gear hob cutters. It is likely that similar results could be achieved with any ferromagnetic material, but the inherent limitation to these types of materials of a BHN based measurement system prevents its use more widely (e.g. outside of traditional tool materials). That said, if a characteristic signal from a non-ferromagnetic material could be measured similarly, it would be worthwhile using the methodology presented here.

Although the BHN profile curves for the different coating thicknesses were clearly separated and reproducible, because they are non-linear it is a limitation of the work that these have to be considered relative values of coating depth and not absolute measurements (e.g. 5 μm has been measured to be less than 10 μm, rather than being absolutely 5 μm). Although the measurements were compared with XRF derived data, further work is required to evaluate the smallest difference in coating depth that the BHN technique can resolve and to then validate the BHN derived coating depths through comparison with direct measurement techniques that can produce absolute values (e.g. metallography).

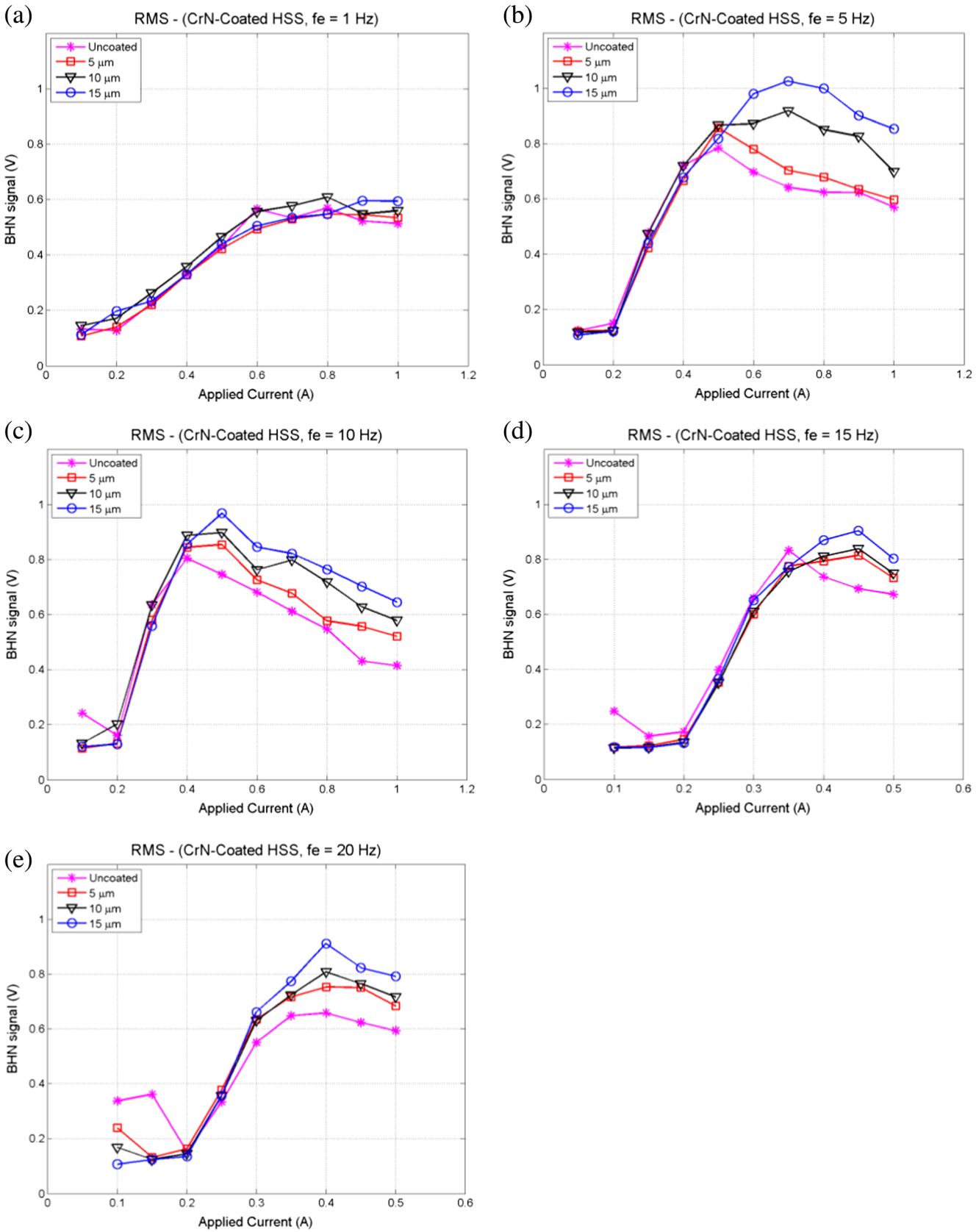

Fig. 8 RMS value of BHN signal measured from CrN coated HSS at **a** 1, **b** 5, **c** 10, **d** 15 and **e** 20 Hz

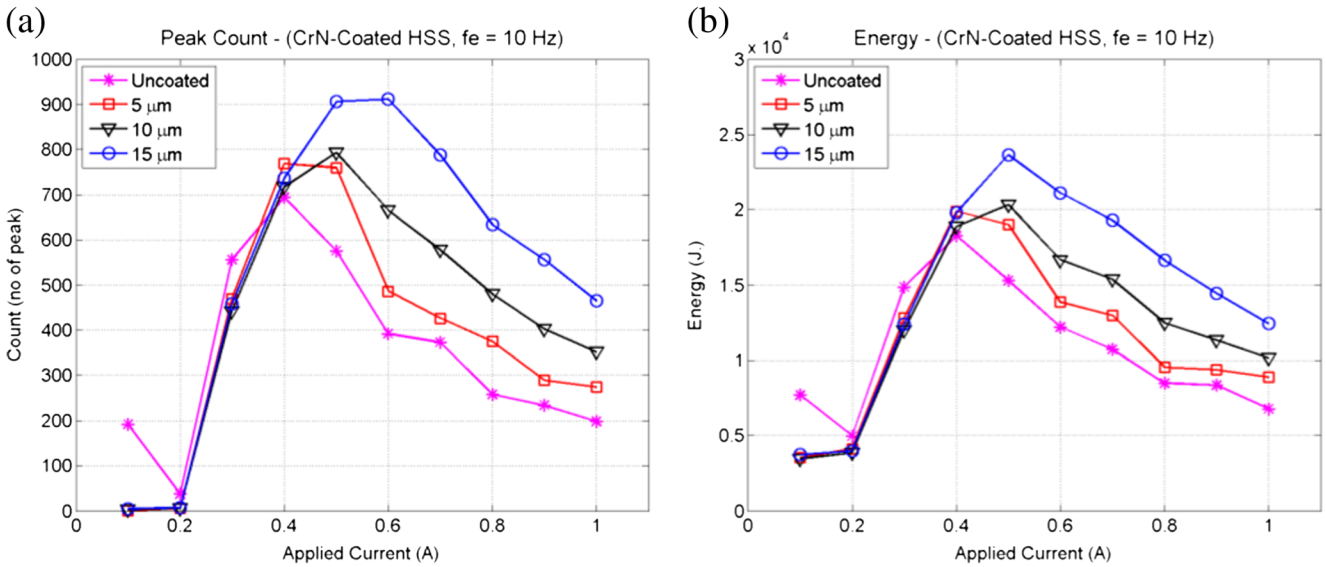

Fig. 9 BHN signal of CrN coated HSS **a** peak count and **b** signal energy

Although this BHN measuring technique has initially been developed to be performed offline during tool change/selection, this non-destructive and quick measuring method can reduce the production costs due to rejected parts caused by tool breakage (e.g. from the unknowing use of an already worn tool that has a remaining tool life less than the planned process) and can also reduce the time lost through unplanned tool replacement during production. The three sensory features of BHN signal in the effective range are monitored both before and after use the cutting tool to know the current coating condition. It is helpful for the operator to be aware when the tool is in highly used condition and avoid using the weakened tool.

Any online, factory ready system developed from the work presented here would need to consider how to repeatedly take useful measurements of the tool considering the potential uncertainty in tool position if the tool is to be moved to a known 'safe' (from chips, coolant) location within the machine for measurement, or the influence of a measurement system integrated into the tool holder on the performance of the tool (tool path, chip formation, coolant, chatter suppression etc.). For the system to be used for a process using multi-point tools consideration would also need to be made towards ensuring the same part(s) of the tool were subjected to the measurement.

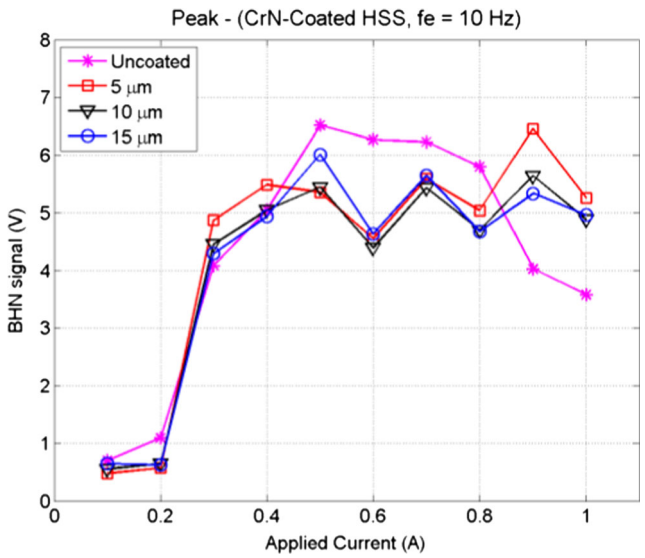

Fig. 10 Peak amplitude extracted from BHN signal of CrN coated HSS at fe = 10 Hz exciting frequency

4 Conclusions

The conclusions of this work were as follows:

- A novel magnetic measuring system based on BHN technique can be used to measure the coated layer of high-speed cutting tool as in a similar fashion to the use of magnetic methods to measure case hardening.
- The proposed BHN system can successfully indicate the thickness of CrN coated HSS where the exciting frequency is equal to 5, 10, 15 and 20 Hz, while only 20 Hz excitation can be used to indicate the thickness of TiN layer coated on HSS specimen.
- The most significant BHN feature used in this study are RMS, peak count, and signal energy, which are extracted from the BHN signal after the RMS profile reach the maximum point. These features can be used individually to indicate the thickness of coating depth very well.

To increase the reliability of the results, the use of multiple BHN features can improve the result accuracy, which is the key concept of the data fusion. As the BHN measurement is

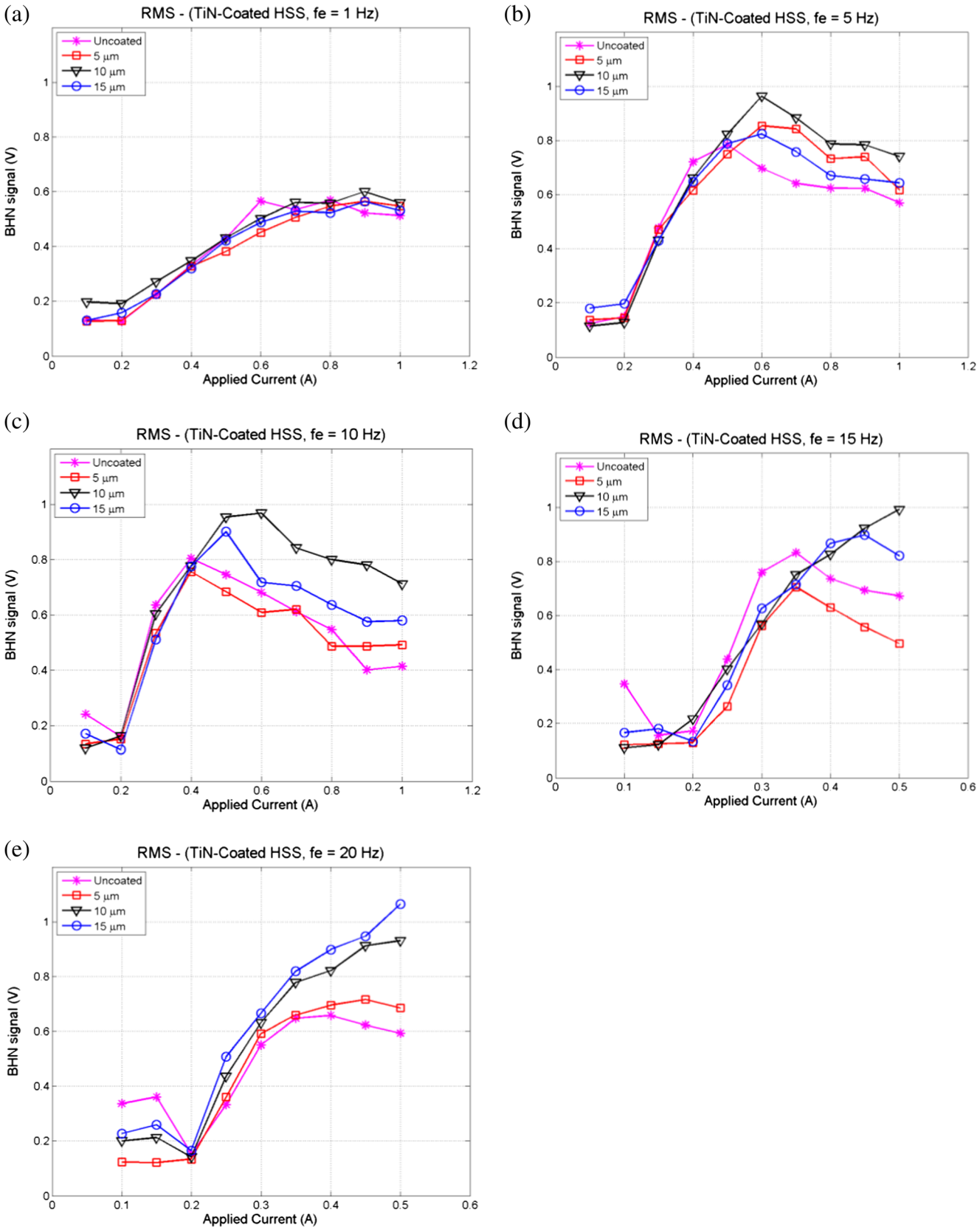

Fig. 11 RMS value of BHN signal measured from TiN coated HSS at **a** 1, **b** 5, **c** 10, **d** 15 and **e** 20 Hz

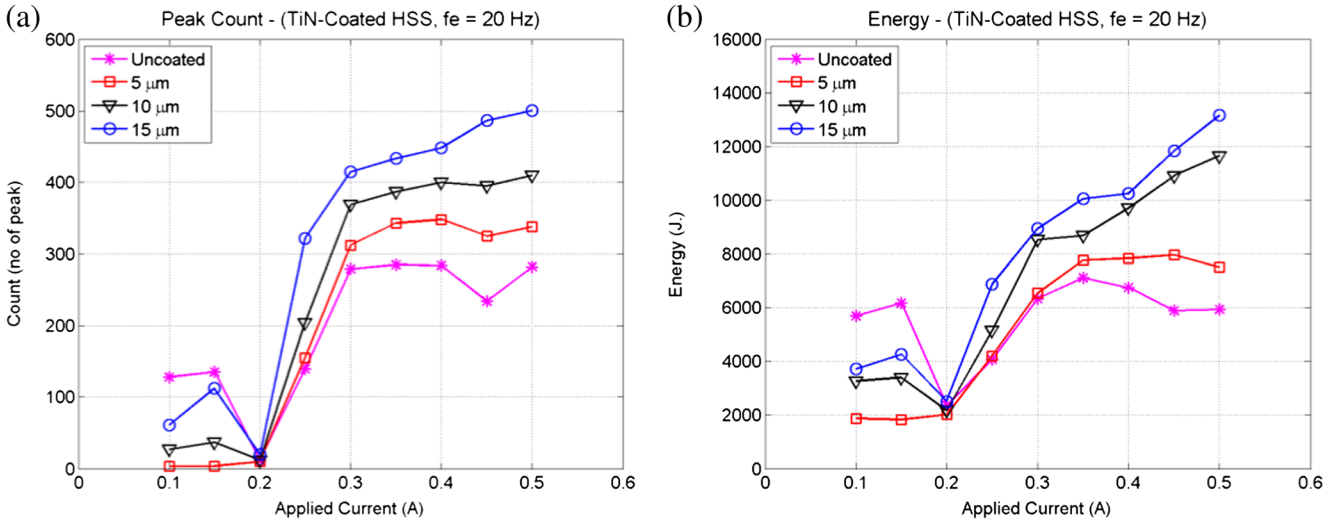

Fig. 12 BHN signal of TiN coated HSS **a** peak count and **b** signal energy

repeatable and considered as accurate and very fast method, the application of BHN technique for coating depth evaluation will be an important issue for the future research on tool condition monitoring.

Acknowledgements The authors acknowledge the financial support provided by the Royal Thai Government for this work.

References

1. Bobzin K High-performance coatings for cutting tools. CIRP Journal of Manufacturing Science and Technology. doi: 10.1016/j.cirpj.2016.11.004
2. Fernández-Valdivielso A, López de Lacalle LN, Urbikain G, Rodriguez A (2015) Detecting the key geometrical features and grades of carbide inserts for the turning of nickel-based alloys concerning surface integrity. Proc Inst Mech Eng C J Mech Eng Sci 230(20):3725–3742. doi:10.1177/0954406215616145
3. Kim DM, Lee I, Kim SK, Kim BH, Park HW (2016) Influence of a micropatterned insert on characteristics of the tool–workpiece interface in a hard turning process. J Mater Process Technol 229:160–171. doi:10.1016/j.jmatprotec.2015.09.018
4. Olovsjö S, Nyborg L (2012) Influence of microstructure on wear behaviour of uncoated WC tools in turning of Alloy 718 and Waspaloy. Wear 282–283:12–21. doi:10.1016/j.wear.2012.01.004
5. Thornton R, Slatter T, Lewis R (2014) Effects of deep cryogenic treatment on the wear development of H13A tungsten carbide inserts when machining AISI 1045 steel. Prod Eng 8(3):355–364. doi:10.1007/s11740-013-0518-7
6. Bushlya V, Zhou J, Ståhl JE (2012) Effect of cutting conditions on machinability of superalloy Inconel 718 during high speed turning with coated and uncoated PCBN tools. Procedia CIRP 3:370–375. doi:10.1016/j.procir.2012.07.064
7. Özbek NA, Çiçek A, Gülesin M, Özbek O (2016) Effect of cutting conditions on wear performance of cryogenically treated tungsten carbide inserts in dry turning of stainless steel. Tribol Int 94:223–233. doi:10.1016/j.triboint.2015.08.024
8. Seemuang N, McLeay T, Slatter T (2016) Using spindle noise to monitor tool wear in a turning process. Int J Adv Manuf Technol 86(9):2781–2790. doi:10.1007/s00170-015-8303-8
9. Duboust N, Melis D, Pinna C, Ghadbeigi H, Collis A, Ayvar-Soberanis S, Kerrigan K (2016) Machining of carbon fibre: optical surface damage characterisation and tool wear study. Procedia CIRP 45:71–74. doi:10.1016/j.procir.2016.02.170
10. Maia LHA, Abrao AM, Vasconcelos WL, Sales WF, Machado AR (2015) A new approach for detection of wear mechanisms and determination of tool life in turning using acoustic emission. Tribol Int 92:519–532. doi:10.1016/j.triboint.2015.07.024
11. Ferrari G, Gómez MP (2015) Correlation between acoustic emission, thrust and tool wear in drilling. Procedia Materials Science 8:693–701. doi:10.1016/j.mspro.2015.04.126
12. Li X (2002) A brief review: acoustic emission method for tool wear monitoring during turning. Int J Mach Tools Manuf 42(2):157–165. doi:10.1016/S0890-6955(01)00108-0
13. Dinakaran D, Sampathkumar S, Sivashanmugam N (2009) An experimental investigation on monitoring of crater wear in turning using ultrasonic technique. Int J Mach Tools Manuf 49(15):1234–1237. doi:10.1016/j.ijmachtools.2009.08.001
14. Yao CW, Chien YX (2014) A diagnosis method of wear and tool life for an endmill by ultrasonic detection. J Manuf Syst 33(1):129–138. doi:10.1016/j.jmsy.2013.05.003
15. Wang C, Ming W, Chen M (2016) Milling tool's flank wear prediction by temperature dependent wear mechanism determination when machining Inconel 182 overlays. Tribol Int. doi:10.1016/j.triboint.2016.08.036
16. Simeone A, Woolley EB, Rahimifard S (2015) Tool state assessment for reduction of life cycle environmental impacts of aluminium machining processes via infrared temperature monitoring. Procedia CIRP 29:526–531. doi:10.1016/j.procir.2015.02.070
17. Moorthy V, Choudhary BK, Vaidyanathan S, Jayakumar T, Rao KBS, Raj B (1999) An assessment of low cycle fatigue damage using magnetic Barkhausen emission in 9Cr-1Mo ferritic steel. Int J Fatigue 21(3):263–269. doi:10.1016/s0142-1123(98)00079-6
18. Vincent A, Pasco L, Morin M, Kleber X, Delnondedieu M (2005) Magnetic Barkhausen noise from strain-induced martensite during low cycle fatigue of 304 L austenitic stainless steel. Acta Mater 53(17):4579–4591. doi:10.1016/j.actamat.2005.06.016

19. Lindgren M, Lepistö T (2000) Application of a novel type Barkhausen noise sensor to continuous fatigue monitoring. NDT&E International 33(6):423–428. doi:10.1016/s0963-8695(00)00011-6
20. Moorthy V, Shaw BA, Mountford P, Hopkins P (2005) Magnetic Barkhausen emission technique for evaluation of residual stress alteration by grinding in case-carburised En36 steel. Acta Mater 53(19):4997–5006. doi:10.1016/j.actamat.2005.06.029
21. Wilson JW, Tian GY, Moorthy V, Shaw BA (2009) Magneto-acoustic emission and magnetic barkhausen emission for case depth measurement in En36 gear steel. IEEE Trans Magn 45(1):177–183. doi:10.1109/tmag.2008.2007537
22. Sorsa A, Leiviska K, Santa-aho S, Lepisto T (2012) Quantitative prediction of residual stress and hardness in case-hardened steel based on the Barkhausen noise measurement. NDT & E International 46:100–106. doi:10.1016/j.ndteint.2011.11.008
23. Hao XJ, Yin W, Strangwood M, Peyton AJ, Morris PF, Davis CL (2008) Off-line measurement of decarburization of steels using a multifrequency electromagnetic sensor. Scr Mater 58(11):1033–1036. doi:10.1016/j.scriptamat.2008.01.042
24. Brinksmeier E, Schneider E, Theiner WA, Tönshoff HK (1984) Nondestructive testing for evaluating surface integrity. CIRP Ann Manuf Technol 33(2):489–509. doi:10.1016/S0007-8506(16)30171-8
25. Santa-aho S, Hakanen M, Sorsa A, Vippola M, Leiviska K, Lepisto T (2014) Case depth verification of hardened samples with Barkhausen noise sweeps. In: Chimenti DE, Bond LJ, Thompson DO (eds) 40th annual review of progress in quantitative nondestructive evaluation: incorporating the 10th international conference on Barkhausen noise and micromagnetic testing, Vols 33a & 33b, AIP Conference Proceedings, vol 1581. Amer Inst Physics, Melville, pp 1307–1314. doi:10.1063/1.4864972
26. Bach G, Goebbels K, Theiner WA (1988) Characterization of hardening depth by barkhausen noise measurement. Mater Eval 46(12):1576–1580
27. Moorthy V, Shaw BA, Brimble K (2004) Testing of case depth in case carburized gear steels using magnetic barkhausen emission technique. Mater Eval 62(5):523–527
28. Vaidyanathan S, Moorthy V, Jayakumar T, Raj B (2000) Evaluation of induction hardened case depth through microstructural characterisation using magnetic Barkhausen emission technique. Mater Sci Technol 16(2):202–208. doi:10.1179/026708300101507550
29. Dubois M, Fiset M (1995) Evaluation of case depth on steels by Barkhausen noise measurement. Mater Sci Technol 11(3):264–267
30. Blaow MM, Shaw BA (2015) Effect of excitation field strength on magnetic Barkhausen noise profile in case carburized EN 36 Steel. In: Oral AY, Bahsi ZB, Ozer M, Sezer M, Akoz ME (eds) 4th International Congress in Advances in Applied Physics and Materials Science, vol 1653. AIP Conference Proceedings. Amer Inst Physics, Melville. doi:10.1063/1.4914212
31. Blaow M, Evans JT, Shaw BA (2005) Surface decarburisation of steel detected by magnetic Barkhausen emission. J Mater Sci 40(20):5517–5520. doi:10.1007/s10853-005-4240-5
32. Stupakov O, Perevertov O, Tomáš I, Skrbek B (2011) Evaluation of surface decarburization depth by magnetic Barkhausen noise technique. J Magn Magn Mater 323(12):1692–1697. doi:10.1016/j.jmmm.2011.01.039
33. Santa-aho S, Vippola M, Sorsa A, Leiviskä K, Lindgren M, Lepistö T (2012) Utilization of Barkhausen noise magnetizing sweeps for case-depth detection from hardened steel. NDT & E International 52(0):95–102. doi:10.1016/j.ndteint.2012.05.005
34. Drehmer A, Gerhardt GJL, Missell FP (2013) Case depth in SAE 1020 steel using Barkhausen noise. Mater Res-Ibero-am J Mater 16(5):1015–1019. doi:10.1590/s1516-14392013005000095
35. Franco FA, Gonzalez MFR, de Campos MF, Padovese LR (2013) Relation between magnetic Barkhausen noise and hardness for Jominy quench tests in SAE 4140 and 6150 steels. J Nondestruct Eval 32(1):93–103. doi:10.1007/s10921-012-0162-8
36. Vashista M, Moorthy V (2013) Influence of applied magnetic field strength and frequency response of pick-up coil on the magnetic barkhausen noise profile. J Magn Magn Mater 345:208–214. doi:10.1016/j.jmmm.2013.06.038